

Optical Manipulation of Microscale Fluid Flow

Nicolas Garnier, Roman O. Grigoriev, and Michael F. Schatz

Center for Nonlinear Science and School of Physics, Georgia Institute of Technology, Atlanta, Georgia 30332-0430, USA

(Received 17 March 2003; published 30 July 2003)

A novel optical method is used both to probe and to control dynamics in experiments on the spreading of microscale liquid films over solid substrates. The flow is manipulated by thermally induced surface-tension gradients that are regulated by controlling the absorption of light in the substrate. This approach permits, for the first time, the measurement of the dispersion relation for the well-known contact line instability; the measurements are compared with theoretical predictions from the slip model for spreading films. The experiments also demonstrate the use of feedback control to suppress instability. These results show that optical control can provide dynamically reconfigurable manipulations of fluid flow, thereby suggesting a general approach for constructing reprogrammable microfluidic devices.

DOI: 10.1103/PhysRevLett.91.054501

PACS numbers: 47.20.Ma, 47.54.+r, 47.62.+q

Countless technological applications depend on precise control of fluid flow at small scales. Examples range from the widely used industrial process of coating [1] to recently developed techniques of microfluidics for chemical and biochemical analysis/synthesis via “Labs-on-a-Chip” [2–5]. Control of flow at small scale can also advance fundamental understanding of many physical systems, for example, permitting the investigation of otherwise unobservable, unstable states and patterns [6]. Manipulating surface tension provides a natural approach to regulating flows at small scale because surface forces, like surface tension, dominate when the surface-to-volume ratio is large. The surface tension at the interface between immiscible fluids (e.g., air/liquid) can be altered by changing the temperature; for pure fluids, the surface tension decreases as the temperature increases. The fluids move when gradients in temperature induce surface-tension differences; this is known as the thermal Marangoni (or thermocapillary) effect. At small scale, even small thermal gradients can cause substantial liquid movement [5]. As a consequence, the thermocapillary effect has been utilized successfully in prototype devices for manipulating tiny quantities of fluid [4,5]. In these devices, temperature variations have been generated with heating/cooling devices (e.g., resistive heaters) placed in physical contact with the fluids.

In this Letter, we describe experiments that use optically imposed surface-tension gradients to explore two fundamental aspects of the well-known contact line instability in the spreading of liquid films [7,8]. In these studies, the films are driven on horizontal solid substrates illuminated with a light beam, Fig. 1. Absorption of the beam in the substrate impresses a thermal pattern, where the local substrate temperature increases with illumination intensity. For sufficiently thin films, the thermal gradients in the substrate are directly transferred to the air-liquid interface, thereby inducing surface-tension gradients that drive the flow. With this novel technique, flow

perturbations with a well-defined structure can be imposed by suitable spatial and temporal modulation of the light intensity. In one series of experiments, the perturbations are used to excite a family of unstable modes as well-defined initial conditions; by monitoring the subsequent time evolution of these flows, the dispersion relation for instability of moving contact lines is measured. In another series of experiments, the perturbations are applied as feedback in response to measurements of the

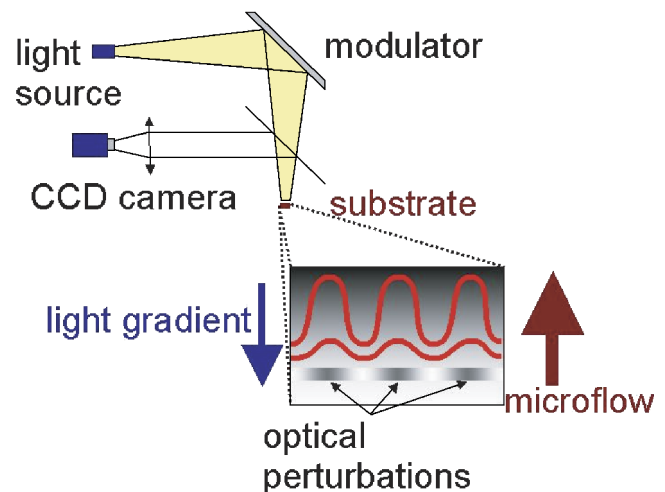


FIG. 1 (color online). Schematic illustration of microflow that is optically driven via the thermocapillary effect. An intensity-modulated beam from a light source illuminates a substrate that supports a tiny quantity of liquid at one end. Temperature variations arise from light absorption and induce surface-tension gradients that drive the flow from the brighter (hotter) to darker (cooler) regions on the substrate. In all experiments, a uniform intensity gradient is applied to produce a temperature gradient of $30\text{ }^{\circ}\text{C}$ per centimeter that drives the flow. In addition, suitable spatial and temporal perturbations of the intensity are employed to probe and to control pattern dynamics.

flow; in this way, suppression of contact line instability via feedback control is demonstrated.

The liquid in our experiments is a commercially available silicone oil (polydimethylsiloxane) with a measured kinematic viscosity of 0.65 S and surface tension of 18 dyn/cm. The bottom surface of a 2.2 cm \times 4.0 cm \times 100- μ m-thick glass substrate is coated with a 20- μ m-thick flat black enamel layer for light absorption, while the substrate's top surface is rendered completely wettable by thorough cleaning with propanol. After cleaning, a thick oil film is applied at one end of the substrate's top surface. Excess oil is then removed by spinning the substrate at a fixed rotation rate for a fixed period of time. This procedure yields a 2.2 cm \times \sim 0.4 cm region that is uniformly coated with a fixed liquid volume of reproducible thickness, as verified by interferometry. The substrate is then placed above a constant-temperature (18°C) heat sink. The substrate is illuminated with light from an arc lamp that is focused into a beam. This beam is modulated at spatial and temporal resolutions characteristic of computer/video displays by devices developed for projection technologies (e.g., Texas Instruments's Digital Micromirror Device). Thermal gradients are measured using an infrared camera (Amber/Raytheon Systems 4-128). The motion of the spreading film is monitored by computer-controlled digitization and processing of video images from high-resolution CCD cameras (Sony XC-77). The film topography is measured *in situ* with interferometry using monochromatic images obtained by narrow bandpass filtering the illumination collected by the camera. Independent determination of the topography by fluorescence emission [9] is performed after the conclusion of some experiments and is found to be in qualitative agreement with the interferometric measurements.

The dynamics of thin films spreading under the action of thermocapillary forces is modeled using the lubrication approximation. In particular, the slip model [10] produces the following nondimensional evolution equation for the film thickness $h(x, y, t)$

$$\partial_t h = \partial_x h^2 - \nabla \cdot [(\alpha h + h^3)(\nabla \nabla^2 h)], \quad (1)$$

where the uniform thermal gradient points in the positive x direction, α is a phenomenological slip coefficient, and all other parameters have been absorbed into the time and length scales. The first and second terms on the right-hand-side of (1) describe, at lowest order, the tangential and normal component of the surface tension, respectively. Both the asymptotic thickness profile $h_0(x + ut)$ achieved under constant flux conditions and the internal solution describing the region of the capillary ridge under the constant volume conditions of the experiment can be obtained by solving the ordinary differential equation

$$h_0''' = (h_0 - 1)(h_0^2 + \alpha)^{-1} \quad (2)$$

subject to the boundary conditions $h_0'(0) = c$, $h_0(\infty) = 1$,

and $h_0'''(\infty) = 0$, where the constant c determines the dynamic contact angle (details are given in Ref. [10]). The asymptotic state $h = h_0$ describes a front solution of (1) moving with velocity $u = 1$ towards negative x . Its stability is determined by (numerically) computing the spectrum $\{\beta_q^n\}$ of the boundary value problem

$$\begin{aligned} \beta_q g = & - \left[\{1 - 2h_0 + (\alpha + 3h_0^2)h_0''\}g + (\alpha h_0 + h_0^3)g'' \right]' \\ & + q^2 [(\alpha + 3h_0^2)h_0'g]' + 2q^2(\alpha h_0 + h_0^3)g'' \\ & - q^4(\alpha h_0 + h_0^3)g, \end{aligned} \quad (3)$$

subject to boundary conditions $h_0''(0)g(0) = h_0'(0)g'(0)$ and $g(\infty) = g'(\infty) = g''(\infty) = 0$. The leading eigenvalue β_q^0 determines the growth rate of sinusoidal disturbances with transverse wave number q . The predictions of the slip model and of a slightly different precursor model [11] regarding both the asymptotic film profile and linear stability of the spreading film are essentially identical, so by comparing these with experimental observations one can test the validity of different assumptions on which both of these models are based.

The free parameters of the model are fitted by use of the experimentally determined thickness profile, Fig. 2(a). In all experiments, the dominant effect of the imposed illumination gradients is to drive spreading of a fixed volume of fluid from coated to uncoated areas of the substrate. In the early stages of spreading, the contact line moves as a front that is uniformly straight transverse to the flow direction. In this case, the film profile in the direction of the flow exhibits the characteristic formation

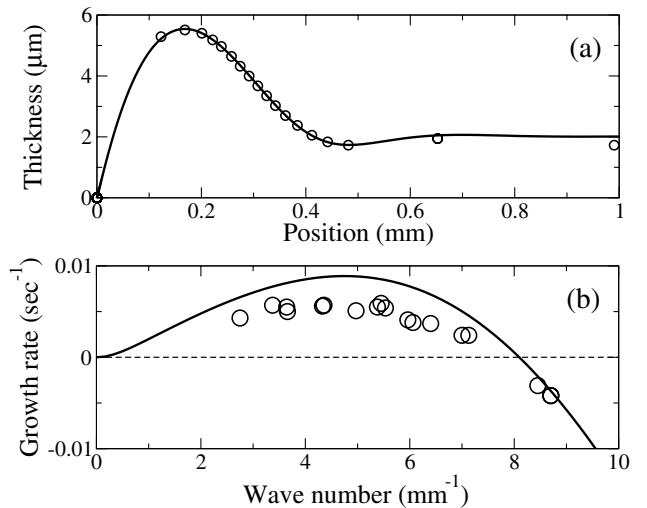


FIG. 2. Experimental measurements (circles) are compared with theoretical predictions (lines) of the slip model for the spreading of thin liquid film on a solid substrate. Error bars on the experimental data are less than the symbol size. (a) The capillary ridge behind the contact line (located at the origin) is the dominant topographical feature of the streamwise profile of an unstable spreading film. (b) The dispersion relation for a spreading film with a profile shown in (a).

of a capillary ridge just behind the contact line [7,11]. As shown in Ref. [10] the profile depends only on a combination of the slip coefficient α and slope c at the contact line as long as $\alpha \ll 1$. We exploit this freedom by choosing $\alpha = 0.01$. The other parameter is then uniquely determined by the location and height of both the local maximum and local minimum [respectively, at positions 0.17 and 0.49 mm in the profile shown in Fig. 2(a)]. The fit gives $c = 2.01 \pm 0.02$ completely defining all free parameters for subsequent comparison of experiments and theory.

In our experiments, an initially straight film front undergoes a dynamic instability leading to the spontaneous formation of parallel rivulets [8]. Stability analysis of (3) shows that the presence of the capillary ridge is responsible for instability of the moving contact line [10,11] and predicts the existence of a range of unstable wave numbers [see Fig. 2(b)], each of which, in principle, can lead to the formation of rivulets. In practice, however, only rivulet states with wave numbers near the maximal growth rate are typically observed [7,8,12]. We use perturbations to study experimentally rivulet modes that would otherwise be unobservable. To examine the behavior of each mode separately, we optically impose a disturbance with a desired wavelength in the transverse direction, Figs. 3(a)–3(c). The optical perturbations, which are localized to the region immediately behind the capillary ridge, are superimposed onto the uniform illumination gradient that drives the mean spreading flow. These perturbations generate a lateral secondary flow that drives fluid from hotter to colder regions; thus, the film depth is periodically modulated transversely near the contact line with the film relatively thicker (thinner) where the illumination is less (more) intense. These thickness variations, in turn, alter the local mobility of the film with the tips (valleys) of the rivulets forming where the contact line advances more (less) rapidly because the film is locally thicker (thinner) [13]. By turning optical perturbations on just long enough to impose a weak disturbance in the film height behind the contact line, we ensure that the nonlinear effects are negligible. After the perturbations are turned off, low amplitude sinusoidal distortions of the contact line are monitored to determine the growth or decay of the rivulet mode.

Comparison of the experimentally obtained dispersion relation with the results of a linear stability analysis based on the slip model presented in Fig. 2(b) shows that the theory predicts well the wave number for maximal growth rate in the experiment. However, the theoretical predictions significantly overestimate the maximal growth rates. The origin of this discrepancy is currently unknown, but it may in part be due to the difference in boundary conditions between theory and experiment: the experiment is conducted with a constant volume of fluid, while the theory assumes constant flux, resulting in somewhat different film profiles behind the capillary ridge as Fig. 2(a) shows.

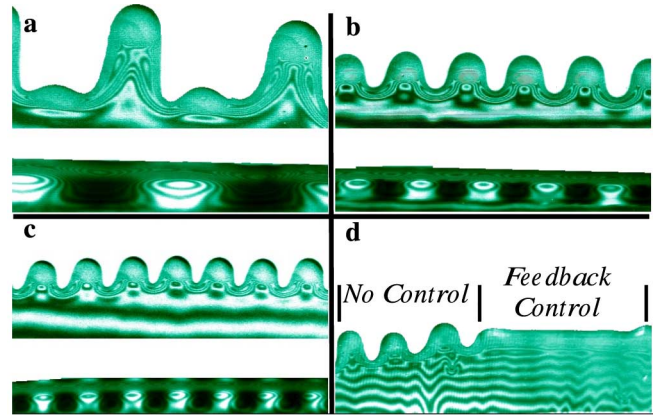


FIG. 3 (color online). Video images under monochromatic illumination show the optical selection and control of thin film flow patterns on horizontal substrates. For each image in (a), (b), and (c), the film pattern is shown at two different times. The lower third of each image displays a thin film whose contact line is initially straight. The film is perturbed with a sinusoidally varying light intensity applied just behind the contact line; this perturbation induces a transverse modulation in the thickness, as indicated by interference fringes. The upper two-thirds of (a)–(c) show the subsequent formation of rivulets in a nonlinear regime at later times after the perturbations have been turned off. In these cases, the intensity variations displayed by the images arise solely from interference fringes, which can be used to measure the film's topography. The pattern wave numbers are (a) 2.60 mm^{-1} , (b) 4.52 mm^{-1} , and (c) 6.17 mm^{-1} . In (d), the contact line instability is suppressed on the right half of a spreading front by feedback via illumination variations applied just behind the contact line. The left half of the (unstable) front evolves in the presence of a uniform constant thermal gradient to form rivulets.

When perturbations with very large wave numbers are imposed, the initial disturbances are observed to decay and are eventually replaced by spontaneously developing rivulets with smaller wave number. Small wave number perturbations are always observed to grow; however, for sufficiently large rivulet spacing, secondary rivulets begin to emerge in the valleys of the original rivulets, Fig. 3(a). This is a consequence of the nonlinear nature of the lubrication Eq. (1) describing the dynamics of the film. Among other effects, nonlinearities couple the dynamics of disturbances with different wave numbers. In particular, the strongest (quadratic) nonlinearities excite the second harmonics of the primary distortion, leading to the formation of secondary rivulets in between the main ones. In Figs. 3(a)–3(c) the phase of the spatially periodic rivulets is observed to differ from the phase of the imposed perturbations; these differences are attributed to the presence of a weak secondary flow transverse to the mean direction of the propagating front most likely caused by a slight nonuniformity in the illumination.

The ability to reconfigure dynamically the driving of the flow is used to confirm a theoretical prediction [10] that the rivulet instability can be completely suppressed using feedback control imposed by applying adaptive

optical perturbations [see Fig. 3(d)]. In these experiments, the position of each point on the contact line is compared with the globally averaged location of the contact line at a given instant. The illumination field that drives the film is perturbed at each transverse location just behind the contact line with an intensity proportional to the local deviation of the contact line from the averaged position. The streamwise profile of the intensity perturbation is constant over a distance comparable to the width of the capillary ridge. The physical mechanisms governing suppression of instability are understood by recognizing that the motion of the liquid film is determined by balancing the imposed thermocapillary force with both the viscous stress and the capillary force arising from the curvature of the free interface. These forces are in equilibrium for a film with a straight contact line and a streamwise profile like that shown in Fig. 2(a). As this equilibrium is unstable, any (even arbitrarily small) spontaneous disturbance will lead to the deviation from the equilibrium profile, which will grow exponentially fast, distorting the contact line. The effect of feedback is to change the stability properties of this equilibrium profile, such that spontaneous disturbances decay rather than grow. In our experiments variations in the local illumination intensity behind the contact line produce gradients in the surface tension that generate secondary flows opposing the spontaneous disturbances. In particular, the streamwise gradients directly change the local speed of the film, either enhancing or suppressing the primary gradient used to drive the flow. The transverse gradients, on the other hand, give rise to secondary flows, which redistribute the liquid under the capillary ridge, changing the mobility of the film and thus providing an indirect stabilizing effect.

Contact line instabilities are commonplace in driven spreading films, arising in cases involving other driving forces, such as gravity [14] and centrifugal effects [15]. We expect that the spreading dynamics could be altered in these cases as well using optically imposed thermocapillary perturbations as the instability mechanism is essentially the same in all three cases. Thus, the optical technique developed for our experiments could potentially be used in many coating applications either to achieve selective patterning or to suppress instability [1,8].

Perhaps most intriguingly, optical microflow control provides a fundamentally new approach to today's rapidly expanding efforts to develop microfluidic devices, such as "Labs-on-a-Chip" for biological and chemical analysis and synthesis [2,3]. Conventional microfluidic systems typically are built using lithographic methods to create fixed networks of microconduits (micropipes), thereby making reconfiguration difficult and creating, effectively, single-use devices [16]. By contrast, our results suggest that "opto-microfluidics" based on optically induced thermocapillarity can drive microflow on substrates that have no moving parts, no microchannels, no electrical

contacts, and no chemical (e.g., hydrophilic/hydrophobic) surface preparations. (In fact, we have performed preliminary experiments, to be reported elsewhere, that show this mechanism may be employed to drive microflow on liquid substrates.) Because the surface-tension gradients that transport microflow can be dynamically changed in response to changing process conditions, as in Fig. 3(d), reconfigurability can be readily incorporated in opto-microfluidics, thereby enabling, in principle, a single device to be "reprogrammed" to perform different fluidic operations in different possible sequences. Such a device would effectively serve as a microfluidic processing unit (μ PU), the fluidic analog of microcomputing's CPU. Finally, it is worth noting that in some cases, the mean temperature field and the temperature gradients could each be optically regulated independently. This capability could be used in the design of certain devices (e.g., for PCR assay) where both flow and thermal process control may be required [17].

Support for this work by the National Science Foundation and the Research Corporation is gratefully acknowledged.

-
- [1] D. P. Birnie, *J. Mater. Res.* **16**, 1145 (2001).
 - [2] G. M. Whitesides and A. D. Stroock, *Phys. Today* **54**, 42 (2001).
 - [3] L. Bousse *et al.*, *Annu. Rev. Biophys. Biomol. Struct.* **29**, 155 (2000).
 - [4] M. Burns *et al.*, *Proc. Natl. Acad. Sci. U.S.A.* **93**, 5556 (1996); T. S. Sammarco and M. A. Burns, *AIChE J.* **45**, 350 (1999).
 - [5] D. E. Kataoka and S. M. Troian, *Nature (London)* **402**, 794 (1999).
 - [6] D. Semwogerere and M. F. Schatz, *Phys. Rev. Lett.* **88**, 54501 (2002).
 - [7] V. Ludviksson and E. N. Lightfoot, *AIChE J.* **17**, 1166 (1971).
 - [8] A. M. Cazabat *et al.*, *Nature (London)* **346**, 824 (1990).
 - [9] M. F. G. Johnson *et al.*, *J. Fluid Mech.* **394**, 339 (1999).
 - [10] R. O. Grigoriev, *Phys. Fluids* **15**, 1363 (2003).
 - [11] D. E. Kataoka and S. M. Troian, *J. Colloid Interface Sci.* **192**, 350 (1997).
 - [12] J. B. Brzoska, F. Brochard-Wyart, and F. Rondelez, *Europhys. Lett.* **19**, 97 (1992).
 - [13] M. P. Brenner, *Phys. Rev. E* **47**, 4597 (1993).
 - [14] J. M. Jerrett and J. R. de Bruyn, *Phys. Fluids A* **4**, 234 (1992).
 - [15] F. Melo, J. F. Joanny, and S. Fauve, *Phys. Rev. Lett.* **63**, 1958 (1989); M. A. Spaid and G. M. Homsy, *Phys. Fluids* **9**, 823 (1997).
 - [16] J. Ruzicka, in *Proceedings of the Micro-Total Analysis Systems 2000 Symposium*, edited by A. van den Berg, W. Olthuis, and P. Bergveld (Kluwer Academic, Dordrecht, 2000), pp. 1–10.
 - [17] L. Waters *et al.*, *Anal. Chem.* **70**, 158 (1998).